The 2009 IEEE/RSJ International Conference on
Intelligent Robots and Systems
October 11-15, 2009 St. Louis, USA

Segmentation and analysis of console operation using self-organizing map with cluster growing method

Satoshi Suzuki and Fumio Harashima

Abstract— **For manipulation of remote mobile robots, adequate scheduling of tasks and selecting of operational commands are required. This paper presents an analysis procedure to make the task switching profile visible by utilizing the Self-Organizing Map (SOM) and new cluster growing method. For practical verification, an experiment system with radio-controlled construction equipments was built, and the proposed analysis procedure was applied to the experimental task. As a result, it was confirmed by correlation analysis that distances among decomposed clusters corresponding to segments of operation strongly relate to performance index of the task.**

I. INTRODUCTION

For an operation of mobile machines, the operator should perceive and recognize the status of an environment and the machine, and has to make operational plans to execute a purpose of work. Hence, analyses of the action and task scheduling of an operator are useful for the design of assistive systems that adapt to any user. For instance, *Therblig* is a practical classification method to analyze the manual operation, and can be applied to the skill analysis [1]. GOMS model [2] for a human computer interaction is other framework to model human cognitive action. A concept of multi-modules and their switching is accepted to explain human control strategy, and the examples are the stochastic switched ARX model (that treats switching of Auto-Regression model with eXogenous input models stochastically and estimates the parameters using an EM-algorithm [3]) and MOSAIC (MOdule Selection And Identification Control [4], that is a comprehensive scheme of human control strategy including the feedforward-feedback learning modules and the switching mechanism of the multiple modules). They are, however, not feasible for an implementation in the machine because they are tools for human analysts. To embed such function into the assistive machine, implementable algorithms that segment human continuous operations are required.

This request comes down to the clustering problem of multivariable time series data involving operator's manipulation and an environmental change, and has to be treated through adequate type of clustering methods. It is difficult for the discriminant analysis (that finds clusters using linear hyper-planes) to obtain precise cluster regions because many hyper-planes are used to form the clusters against the multi-dimensional data. The k-nearest neighbor method is a better method than discriminant analysis; however, a large amount of computations is required for large data set because the search is executed using whole structure of all data set. To avoid this computational problem, a complex procedure, such as combination with tree search, has to be used [5]. Fuzzy clustering is the alternative methods, but there may be little information useful for analysis after the clustering because it does not consider intrinsic property of the target data, such as topological information. In the present study, therefore, an analytical procedure utilizing the Self-Organizing Map (SOM) [6] was adopted. Since the SOM technique makes cluster regions on a two-dimensional map by conserving the topological information, this method is adequate for clustering of the multi-dimensional time series data of a machine operation.

After the trained SOM is obtained, a method to find cluster region is required. U-matrix method is a popular and effective way to make the SOM clusters visible; however, it tends to miss finer structure in complicated data because of averaging computation over neighbors [7]. As other method, the gravitational method [8] is useful to help manual cluster extraction. The data topology visualization method on the SOM grid [9] is also effective to investigate clusters obtained from the trained SOM. These methods are, however, visualization techniques rather than discrimination methods of the clusters, and are still inadequate for implementation to machines. Moreover, if the number of clusters can be estimated beforehand, it is desirable to search the clusters by using the preliminary information to prevent small but significant clusters from missing.

The main contribution of the present paper is to propose new clustering method for the SOM that can treat ill-conditioned data of machine operations. The effectiveness was verified by applying to the remote operational task. Moreover, the learning process of the operator was investigated using the proposed method, and the skill transition of the operator was analyzed. An organization of this paper is as follows. Section II explains a human-control model for a remote machine operation and proposes the SOM analysis procedure with the new cluster growing method. In Section III, a remote operation experiment system and the test are described. Section IV shows the experimental result and the SOM analysis. Last Section V mentions the conclusions and discussions.

This work is supported by a Grant-in-Aid for Scientific Research (A) of the Japanese Ministry of Education, Culture, Sports, Science and Technology.

S. Suzuki is with School of Science and Technology for Future Life, Department of Robotics and Mechatronics, Tokyo Denki University, 2-2 Kanda-Nishiki-cho Chiyoda-ku Tokyo 101-8457, Japan ssuzuki@fr.dendai.ac.jp

F. Harashima is with Tokyo Metropolitan University, 1-1 Minami-Osawa Hachioji-Shi, Tokyo 192-0397, Japan f.harashima@ieee.org

II. Segmentation of operation

A. Human processing model and its application to SOM

An operator of remote machines must cope with unpredictable events from exogenous factors since the circumstance around the machine changes as the machine moves. Hence, for evaluation of the operator's ability, status of the circumstance should be considered. Specifically, user cognitive processing appears to be induced by the following statuses: the machine status (M-status), the environment status (E-status), and the task substance (T-status). A human can be treated as a controller that receives the MET-statuses s and outputs the operational commands ρ, as shown in Fig. 1, where s is described as $s := [\ q^T\ p^T\ ]^T$ using the machine-environment variable q and the T-status variable p.

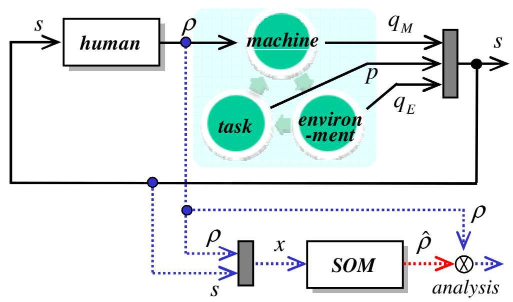

Fig. 1. Model of human on a remote machine operation, and the SOM analyzer

The input vector x for the SOM training is defined as follows using s and the operator's command $\rho \in \mathcal{I}$.

$$x[t] = [\ \rho[t]\ s^T[t]\ ]^T, \tag{1}$$

where $t \in \mathcal{N}$ is the sampling counter. Maximum of t, *i.e.*, final time, is described as T. A SOM technique conduces to clusters that correspond to the similar input vector x onto a two-dimensional lattice of points by iterative update computation of the reference vector $m_i \in R^N (i = 1 \cdots L)$ [6], where N is the size of the vector x, and L is total amount of nodes of the SOM lattice. The node that is closest to $x[t]$ is called the "best-matching node", c, and is defined as

$$c[t] = arg \min_i \{\|x[t] - m_i\|\},\ i = 1, 2 \cdots L. \tag{2}$$

The set of the node n_i that involves the reference vectors m_i is called map $M = \{n_i\}$, where $i = 1, 2 \cdots L$. In the present study, a rectangular map with hexagonal topology was adopted, and u and v were described as coordinate variables for the horizontal right and vertical down directions, respectively. There are two reasons for a choice of hexagonal topology: 1) it is popular in SOM applications and it is easy to be confirmed visually [13], and 2) there is less skew in distance between two nodes on the planer map regardless of the direction. Conversion from the node number i to the node coordinate value (u, v) is given by $i \mapsto (i - u_{dim}(v-1),\ \lfloor (i-1)/u_{dim} \rfloor) =: (u, v)$, where u_{dim} and v_{dim} are the horizontal and vertical sizes of the lattice, and the notation of $\lfloor\ \rfloor$ is a floor function. The node located at (u, v) is described as node-(u, v), and the corresponding reference vector is described as $m(u, v)$ below.

B. Cluster growing method

In the present authors' previous study, it was confirmed that the command prediction by the trained SOM was relatively good (at 65% - 74% by the 1st - 5th predictions); however, an objective analysis concerning clusters had been insufficient. That was because it was difficult to find boundaries of clusters since conditions of the remote machine operation differed from usual SOM applications in the following respects.

- The input vector contains discontinuous time series data that change always; meanwhile, the usual SOM deals with static discrete data.
- The input vector includes illegal data due to the erroneous or unskilled operation.

These issues prevent clusters from forming clearly even if the number of the repetition in training computation is increased. Alternatively in this present study, a method of a cluster growing from seeds that are termed "cluster core" is presented. This approach utilizes continuity of a SOM elastic net to find the core and forms the clusters. Since the map M is considered as a type of manifold that is spanned by the reference vectors, a gradient of the reference vector, ∂m, can be computed by referring the node location on the two-dimensional map. The nodes of which $\partial m(i, j)$ are small can be considered as candidates of the cluster cores. The remaining procedure is to grow the core and to decide the boundaries of region after adequate candidates of the core have been decided. The details are below.

1) Computation of gradient: Variation of the reference vector at each node is computed along the lattice. Assuming the directions of lattice are termed a, b, and c as indicated in Fig. 2, six partial gradients of the reference vector $m(i, j)$ corresponding to the node-(i, j) is computed as

$$\begin{aligned}
\partial m(i,j)/\partial a_\pm &:= m(i \pm 1, j) - m(i, j),\\
\partial m(i,j)/\partial b_+ &:= m(i + 1, j - 1) - m(i, j),\\
\partial m(i,j)/\partial b_- &:= m(i, j + 1) - m(i, j),\\
\partial m(i,j)/\partial c_\pm &:= m(i + 1, j \pm 1) - m(i, j).
\end{aligned}$$

Gradient $\partial m(i, j)$ is obtained as the average of above-mentioned partial gradients:

$$\partial m(i,j) := \frac{1}{6} \sum_* \left\| \frac{\partial}{\partial *} m(i,j) \right\|, * = \{a_+, a_-, b_+, b_-, c_+, c_-\}. \tag{3}$$

Gradient values $\partial m(i, j)$ computed at all nodes are stored into the (i, j)-element of newly defined gradient array $\partial M \in \mathcal{R}^{u_{dim} \times v_{dim}}$. At that time, the gradient computation at edges of the rectangular map was eliminated because the measure space around the edge is skewed; hence, $\partial m(i, j)$ is computed at the range of $i = 2, 3, \cdots, (u_{dim} - 1), j = 2, 3, \cdots, (v_{dim} - 1)$.

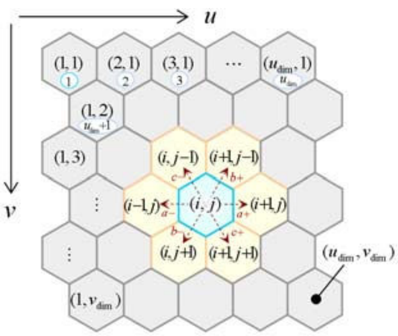

Fig. 2. SOM lattice and its coordinate system

2) Extraction of cluster cores: The number of clusters $K \in \mathcal{N}$ that we want to find is specified at first. After sorting $\partial m(i,j)$ in ascending order, the top K nodes are selected as the cluster cores. If a distance from one core to other is short, it is believed that the two cores are included to same cluster, and other new core is chosen from the sorting list. Specifically, using a threshold δ_1, the node-(i', j') that satisfies $\|[i,j]^T - [i',j']^T\| < \delta_1$ is not chosen as a core. For the next step, the cluster number k is stored in the element (i,j) of the prepared cluster array $C \in \mathcal{I}^{u_{dim} \times v_{dim}}$, where all elements of C are initialized to zero at first.

3) Growing of the clusters: Regions of clusters are expanded from the cores. Focusing on one of the cores and checking the peripheral area around the chosen core, the peripheral area is added to the original cluster region when the difference between the original region and the peripheral area is small. Hereinafter, the details is concretely described:

1) The element storing value of k is extracted from C, and the mask pattern C_B is computed by a logical operation, $C_B = C \cap k$.
2) An eight neighbor dilation creates a mask C_D from C_B.
3) Region C_C of a contour around the cluster-k is extracted by $C_C = C_D - C_B$.
4) The search node is selected from nodes that have element "1" in C_C. If the value of a gradient at the search node is larger than a pre-determined threshold, other search node is selected again by checking elements of C_C, because the first search node is considered as a boundary of clusters.
5) An eight neighbor pattern around the search node, C_{Cns}, is prepared.
6) A logical set S_P is computed by a logical product operation against the original mask C_B using C_{Cns}.
7) All reference vectors m_P of the nodes that have element "1" in S_P is compared with the other reference vector m_{Ccn} of the present search node-$(i_{Ccn}, j_{Ccn})_k$. If $\|m_{Ccn} - m_P\| < \delta_2, {}^{\exists} m_P \in S_P$, it is decided that the search node is a part of the cluster-k, and the cluster number k is recorded in a $(i_{Cnc}, j_{Cns})_k$-element of the cluster array C, where δ_2 is small threshold parameter.
8) Other search node is selected again, and return to step 4). If above-mentioned processing was finished against all search nodes, the cluster counter is increased as $k \rightarrow k+1$, and return to step 1).
9) If the step 8) has finished for all K cluster cores, return to step 1).
10) All procedure is terminated when a search node for all K clusters does not remain.

III. Remote Operation of Radio Controlled Construction Equipments

A. Experimental set up

The task is a basic soil excavation. Wireless cameras on the excavator and the truck captured video images, and displayed on monitors for the operator, as shown in Fig. 3(a). The operator manipulated both the excavator and the truck at one's own discretion. Figure 3(b) shows the overview of the work area. The field consists of the motorable road, the restricted area, three drilling sites, and one unloading site. The excavator and truck were put at their starting position at the beginning of trial. The operator moved the machines to the drilling site, collected the sample pieces with the excavator, loaded the pieces on the truck bed, and carried them to the unloading site by the truck. Requests, such as 'the total trial time as short as possible', 'the number of samples as large as possible', and 'the number of trouble as small as possible', were asked to the participant. The participant was also instructed to improve the performance index $J = \frac{1500}{T_t} + \frac{S}{12}$ in order to encourage an enhancement of the skill, where T_t and S are the total time of one trial and the total number of the collected sample pieces, respectively.

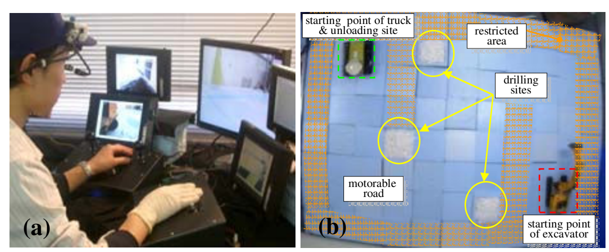

Fig. 3. Remote operation console (a), and overview of the work area (b).

Positions and directions of the excavator and truck were computed using the detected positions of the LEDs attached to them. Compensation for optical distortion was performed offline using MATALB with Weng model [10]. An angle of the excavator's boom and a rotation of the superstructure were measured by potentiometers. The measured signals were transmitted by wireless and recorded. Operations of switches of the console were also recorded. The sampling frequencies of the video images and analog signals were 30 fps and 1 kHz, respectively.

B. Operational Command

Crawler velocities for the excavator and the truck was controlled by two sliders with hands. The velocity commands were converted into the crawler operation mode κ_c as $\kappa_c = \{0\,(stop),\ 1\,(forward),\ 2\,(left\ f.\ steer),\ 3\,(left\, pinwheel),$

4 ($right\ b.\ steer$), 5 ($backward$), 6 ($left\ b.\ steer$), 7 ($right\ pinwheel$), 8 ($right\ f.\ steer$) }, where "*f.*" and "*b.*" are abbreviations of "forward" and "backward", respectively[10]. The bucket arm is manipulated by two cross levers, and the operator commands consisted of the superstructure rotation mode; ${}^e\kappa_r := \{0 : stop,\ 1 : left\,rotation,\ 2 : right\,rot.\}$, the arm mode; ${}^e\kappa_a := \{0 : stop,\ 1 : arm\ bend,\ 2 : arm\ stretch\}$, and the bucket mode; ${}^e\kappa_b := \{0 : stop,\ 1 : boom\ up,\ 2 : boom\ down\}$, respectively. The excavator's bucket arm operation mode ${}^e\kappa_h$ is obtained as ${}^e\kappa_h := (3^2)\cdot{}^e\kappa_r + (3^1)\cdot{}^e\kappa_a + (3^0)\cdot{}^e\kappa_b$. Finally, all operation modes, that consist of the truck crawler modes ${}^t\kappa_c \in \{0 \sim 8\}$, the excavator crawler modes ${}^e\kappa_c \in \{0 \sim 8\}$ and the excavator shovel operation mode ${}^e\kappa_h \in \{0 \sim 27\}$, are summarized into one variable ρ as

$$\rho(t) := 1 + {}^t\kappa_c + ({}^e\kappa_c \wedge 1)({}^e\kappa_c + 8) + ({}^e\kappa_h \wedge 1)({}^e\kappa_h + 16), \tag{4}$$

where superscripts of "t" and "e" denote the truck and the excavator, respectively.

C. Elements Selection for MET-vector

For this soil excavation, not only position/posture of the equipments but also the geographical relation to the digging sites/no restricted area should be considered. Hence, machine-environment vector q was chosen as follows [11].

$$\begin{aligned} q \;&:=\; [\ q_1^T\ q_2^T\ q_3^T\ ] \quad \in \mathcal{R}^{27} \qquad (5)\\ &q_1 := [\ {}^t(d_{f330}\cdots d_{f210}), {}^e(d_{f330}\cdots d_{f210})\ ]^T\\ &q_2 := [\ {}^td_s,\ {}^ed_s,\ {}^t\xi_s,\ {}^e\xi_s\ ]^T \quad \in \mathcal{R}^{12}\\ &q_3 := [\ {}^td_e,\ {}^t\xi_e,\ {}^eh_b\ ]^T \quad \in \mathcal{R}^3, \end{aligned}$$

where $d_{f\theta}$ is a distance from the equipment to the restricted area in a direction of θ $[degree]$ from the traveling direction of the crawler, ${}^td_s({}^ed_s)$ is a distance vector from the truck (excavator) and the center of each digging site, ${}^t\xi_s({}^e\xi_s)$ is similar vector of relative angles, ${}^td_e$ and ${}^t\xi_e$ are the distance and relative angle from the truck to the excavator's crawler, and ${}^eh_b$ is a height clearance between the excavator's bucket fork and the truck bed, respectively. The task status p was defined as $p := \{0 : no\,payload,\ 1 : payload\ on\ bucket,\ 2 : payload\ on\ truck\ bed\}$ using the payload status.

IV. Experimental results and SOM analyses

A. Operational Performance

Written consent and ethical approval of 10 participants, aged 21 to 23 yrs were obtained before the examinations. At least three trials were repeated for three days, hence the total were 9 or 10 trials. For the SOM analysis, one participant was chosen among ten participants because all data during ten trials without abnormal detection of markers could be recorded in only case of the participant. Figure 4 shows improvement of T_t, S, and J. The total trial time T_t indicates decreasing since the gradient and the correlation factor of the regression line are -0.44 and 0.75, respectively. Both the sum of samples S and the performance index J demonstrate an upward trend. Checking recorded movie, the digging operations at the third and the eighth trials were not smooth. Especially, at the third trial, the participant tried to dig samples wrongly four times (normally, three times). The inadequate operation appears to have affected the low performance index at the third and eight trials.

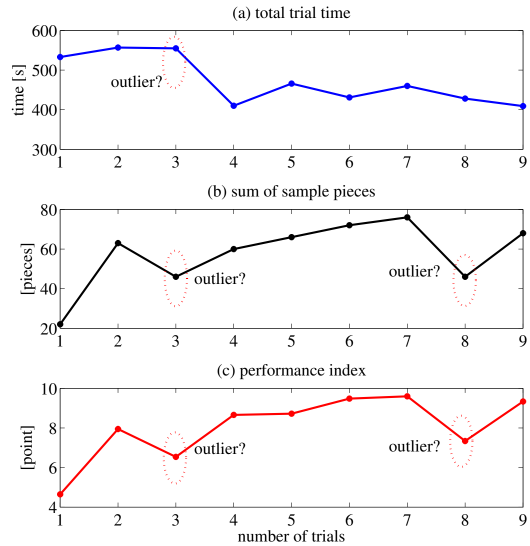

Fig. 4. Improvement of the task time T_t (a), the collected sample pieces S (b), and the performance index J (c)

B. Clustering of operation by SOM

The computation of the SOM was performed using the SOM_PAK [12]. Each component of the input vector x was normalized into the $[-1, 1]$ range by using the maximum and minimum values of the time series data at the ninth trial. Data of other trials were normalized similarly by using the same scale parameters. Since it is preferable for the horizontal and vertical sizes of the rectangular map to be chosen in proportion to the ratio of two square roots of the first and second maximum eigen-values of the covariance matrix $\{x\}\{x\}^T$ [13], the size of the SOM lattice were decided as $u_{dim} = 45$ and $v_{dim} = 30$ (the average ratio of all nine trials was 1.4999, and the rage of σ_1/σ_2 was $1.1770 \sim 1.842$). A bubble type was chosen for a neighborhood kernel function. On the learning process, a fine tuned computation was performed after the rough tuned one was computed. The learning rate & learning length were specified as 0.05 & 2000 and 0.02 & 1.5 million, respectively, so as to meet such requirement that the learning length is more than 500 times of the number of nodes [6]. The number of search clusters was specified as $K = 25$ because the 16 operational modes, as shown in Table I, and 9 margins were considered. Thresholds for the cluster growing were chosen as $\delta_1 = 6$ and $\delta_2 = 0.5$ by checking the obtained several maps.

As an example, the gradient map for the ninth trial is shown in Fig. 5(a). The blue (red) area indicates a low (high) gradient node. The boundary curves can be found, and some clusters surrounded by the curve are confirmed. There is, however, ambiguous area of which boundary is unclear, and it is difficult to objectively segment such area into clusters. Figure 5(b) shows a distribution of the cluster cores that were detected by the proposed method. Colors of the cluster cores were changed in the figure from blue to red according to the order of emerging in time series. It can be confirmed that their nodes are put on by keeping the relatively sufficient distance. The final result of the growing clustering using those cluster cores is shown in Fig. 6. Comparison between the left in Fig. 5 and Fig. 6 demonstrates that blue areas in the original gradient map were segmented adequately as clusters.

The clustering method proposed here satisfies an *internal cohesion* condition because of the growing from one point by iteration of the dilation. In addition, an *external isolation* condition is also satisfied since termination of the growing search is decided by checking absolute values of the node's gradients; hence, the present method appears adequate for segmentation of the operational behavior.

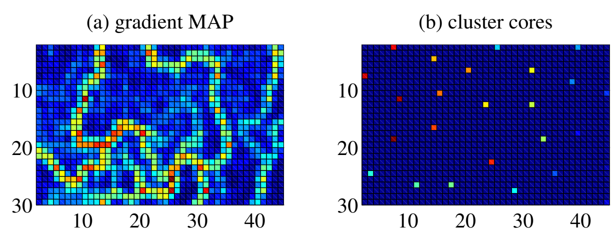

Fig. 5. Gradient map (a), and cluster cores (b)

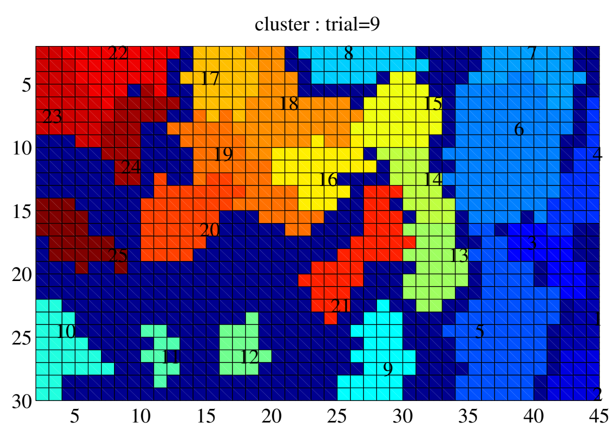

Fig. 6. Segmented clusters of manipulation for 9th trial

C. Relational analysis between manipulation and clusters

Finding the input vector x that is a best matching to the reference vector m of the segmented cluster core, manipulations corresponding to the cluster are summarized to Fig. 7. Numbers described in the vertical direction indicate the cluster numbers according to the order of the emergence. Abbreviation labels used in Fig. 7 are explained in Table I. In the figure, the label colored by red indicates that a type of the manipulation was unclear. The yellow labels

TABLE I

LABELS OF THE REMOTE OPERATION TASK AND ITS MEANINGS

label	meanings
T/A-*	truck approach to the *-drilling site
E/A-*	excavator approach to the *-drilling site
T/P-*	truck positioning around the *-drilling site
E/P-*	excavator positioning around the *-drilling site
E/D	excavator digging
E/L	excavator loading of the payload
T/T	truck transport with the payload
T/U	truck unloading of the payload

(*=1,2,3 : the drilling site number)

denote multiple clusters that were assigned with same type of manipulation. Checking the recorded video of the experiment, manipulations corresponding to the yellow-labeled clusters included operational errors, minor accidents, and trial-and-errors; hence, such troubles appear to be responsible for the inadequate clustering. On the other hand, the blue-labeled clusters are same type of manipulation but differ in terms of the work places. Lowercase characters were added in their labels for discrimination of clusters when one manipulation was segmented into more than two clusters. The green-labeled cluster denotes one cluster that included more than two different types of manipulations. Existence of the blue- and green-labeled clusters may give suggestions that the difference of the work place and the particle size of the SOM analysis should be taken into consideration to enhance the analysis of the clustering. The figure shows that the inadequate clusters reduced as the trial increased. Except above-mentioned essentially inadequate cases, the segmented clusters could match actual subtask reasonably, and the proposed algorithm appears to work well.

cluster no	number of trials: 1	2	3	4	5	6	7	8	9
1	T/A-1, no E/A-1	E/A-1	E/A-1	T/A-1a	E/A-1	E/A-1a	E/A-1	T/A-1a	E/A-1a
2	T/A-1a	T/A-1	T/A-1a	T/A-1b	T/A-1	E/A-1a	E/P-1	T/A-1b	E/A-1b
3	T/A-1b	T/P-1	T/A-1b	T/A-1c	E/P-1	T/A-1	T/A-1	T/P-1	E/A-1c
4	E/P-1	E/D-1	T/P-1	T/P-1	E/D-1	T/P-1	T/P-1	E/D-1	E/A-1d
5	E/D-1	E/D-1	T/T	E/A-1a	E/L-1	E/P-1	E/D-1	E/D-1	E/P-1
6	E/D-1	E/L-1	T/A-2	E/A-1b	T/T, no T/U	E/D-1	E/D-1	E/L-1	T/A-1
7	E/L-1	T/T	E/D-1?	E/A-1c	E/A-2	T/P-1a	E/L-1	E/L-1	T/A-1
8	T/Ta	T/U	E/A-2a	E/P-1	T/A-2a	T/P-1b	T/Ta	T/T	T/P-1
9	T/Tb	T/A-2	E/A-2b	E/D-1	T/A-2b	E/L-1	T/Tb	T/U	E/D&L-1
10	T/Tc	T/P-2	T/A-2?	E/D-1	T/A-2c	T/T	T/U	E/A-2	T/T
11	T/U	E/D-2	T/P-2?	E/L-1	T/P-2	T/U	E/A-2a	E/P-2	T/U
12	T/A-2	E/D-2	E/D-2	T/T	E/D-2	E/A-2	E/A-2b	T/A-2	E/A-2
13	E/A-2	E/D-2	E/D-2	T/U	E/D-2	E/A-2	E/A-2c	T/P-2	T/A-2a
14	E/D-2	E/D-2	E/D-2	E/A-2	T/P-2	E/P-2	T/A&P-2	E/D-2	T/A-2b
15	E/D-2	E/D-2	T/A-2	T/A-2a	E/L-2	T/A-2	E/D-2	E/D-2	T/A-2c
16	E/L-2	E/L-2	T/P-2	T/A-2b	T/T, no T/U	T/P-2a	E/L-2	E/L-2	T/A-2d
17	T/Ta	T/T	E/D-2	T/P-2	E/A-3	T/P-2b	T/T&U	T/Ta	T/P-2
18	T/Tb	T/T	E/L-2	E/D-2, no E/L, T/T, T/U	T/A-3a	E/D-2	E/A-3	T/Tb	E/D-2
19	T/U	T/U	E/L-2	T/A-3	T/A-3a	E/L-2	E/P-3	T/U	T/P-2
20	T/A-3a	T/A-3	T/T	E/D-3	T/A-3b	T/T	T/A-3	E/A-3	E/L-2
21	T/A-3b	T/P-3	T/A-3	E/D-3	E/D-3	T/U	T/P-3a	E/P-3	T/T
22	T/P-3	E/D-3	E/D-3	E/L-3	E/P-3	E/A-3	T/P-3b	E/T-3	E/D-3
23	E/D-3	E/D-3	E/L-3	E/L-3	E/D-3	E/P-3	E/D-3	E/D-3	E/L-3
24	E/D-3	E/L-3	E/L-3	E/T	T/T	E/D-3	E/L-3	E/L-3	T/T
25	E/L-3, no T/T	T/T	T/T	E/L	T/U	T/U	T/T	T/T	T/U

Fig. 7. Meanings of the segmented clusters

D. Transition analysis of clusters

Investigation of transition in an operator's skill was tried using the presented clustering method. It reasoned that independence among the clusters would increase because the skilled operator switched manipulation adequately and quickly according to a change of the MET-status. To confirm this assumption, similarities of clusters were investigated by computing distances between clusters. Using the group average defined as

$$d(C_i, C_j) := \frac{1}{n_1 n_2} \sum_{m_i \in C_i} \sum_{m_j \in C_j} \|m_i - m_j\|, \qquad (6)$$

the distance $d(C_i, C_j)$ $(i \neq j)$ between clusters C_i and C_j was computed, where n_1 and n_2 are the number of nodes of the clusters C_i and C_j, respectively. Since a minimum distance between a cluster and others can be considered as an index for dependency of the clusters, the minimum distance d_k around the cluster-k, which was computed as $d_k := \min_{\forall i \neq k}(d(C_k, C_i))$, were investigated. Figure 8 shows transitions of the average / variance of 25 d_ks of all clusters. The average roughly increases, and the maximum was given at the seventh trial. It is interesting that the transition pattern of the average resembles the other pattern of the performance index J shown in Fig. 4(c). Actually, the correlation factor r_1 between the average and the performance index was relatively large at 0.7736. Concerning the variance of d_k, the correlation factor against the performance index was also relatively large at 0.7049. The positive correlations demonstrate that a good or ill clustering of the manipulation involves strongly in the task performance.

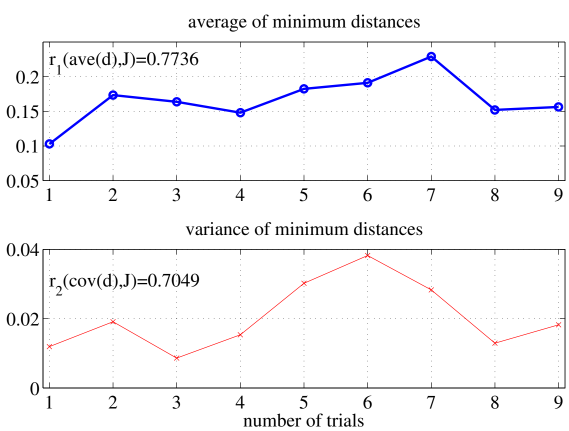

Fig. 8. Transition of clusters' distance

V. Conclusion

To make the task scheduling on manipulation of remote machines visible, a procedure to segment the manipulation was proposed using a SOM technique. Applying the proposed method to a remote operation test proved that characteristics about the segmented clusters could evaluate the skill level of the operator. New clustering method to classify the ambiguous SOM clusters was presented, and it was confirmed the method works well.

Several issues, however, remain. The present analysis did not pay attention to an automated discrimination of faulty manipulation; hence, the reliability to the actual application is not yet sufficient. Since selection of variables for the input vector to the SOM analysis was subjective, the selected input vector was not completely assured to give rich information to the SOM training. Unfortunately in the present analysis, data from only one participant were used due to failure in the data measurement; hence, a statistical verification using all participants data is required after improvement of the experiments. In addition, other type SOM like the sphere SOM has to be considered for enhancement of the analysis quality. These points would be treated in future work.

References

[1] B. Price, "Frank and Lillian Gilbreth and the Motion Study Controversy, 1907-1930," A Mental Revolution: Scientific Management since Taylor, Daniel Nelson, ed. The Ohio State University Press. 1990.

[2] W.D. Gray, B.E. John, and M.E. Atwood, "Project Ernestine: Validating a GOMS Analysis for Predicting and Explaining Real-World Tasks Performance," *Human-Computer Interaction*, vol. 8, pp 237-309, 1993.

[3] T. Suzuki, S. Sekizawa, *et al.*, "Modeling and Recognition of Human Driving Behavior based on Stochastic Switched ARX model," in *Proc. of the 44th IEEE Conference on Decision and Control, and the European Control Conference 2005 (CDC/ECC2005)*, Seville, Spain, pp. 5095-5100, 2005.

[4] D.M. Wolpert, and M. Kawato, "Multiple paired forward and inverse models for motor control," *Neural Networks*, vol. 11, pp 1317-1329, 1998.

[5] C. M. Bishop, "Pattern Recognition and Machine Learning," Springer, 2006.

[6] T. Kohonen, "The self-organizing map," *Proc. of the IEEE*, vol. 78, no. 9, pp 1464-1480, 1990.

[7] E. Merényi and A. Jain, "Forbidden magnification ? II," in *Proc. of 12th European Symposium on Artificial Neural Networks (ESANN)*, Bruges, Belgium, D-Facto, pp.57–62, 2004.

[8] D. Merkl and A. Rauber, "Alternative ways for cluster visualization in Self-Organizing Maps," in *Proc. of 1st Workshop on Self-Organizing Maps (WSOM97)*, 1997.

[9] K. Tasdemir and E. Merényi, "Data topology visualization for the Self-Organizing Map," in *Proc. of European Symposium on Artificial Neural Networks (ESANN)*, Bruges, Belgium, pp.277–282, 2006.

[10] S. Suzuki, and F. Harashima, "Skill analysis focused on the hand discrete movement for machine manipulation," in *Proc. of the 13th IEEE Int. Conf. of Emerging Technologies and Factory Automation (ETFA2008)*, Hamburg, Germany, pp 156–163, 2008.

[11] S. Suzuki, "Visualization of task switching strategy of machine operation," *in the 2009 IEEE International Conference on Networking, Sensing and Control (ICNSC2009)*, Okayama City, Japan, pp.156–163, 2009.

[12] http://www.cis.hut.fi/research/som_lvq_pak.shtml

[13] T. Kohonen, Self-Organizing Maps, *Springer-Verlag*, Heidelberg Berlin, 1995.